Generation of singlet oxygen at room temperature mediated by energy transfer from photoexcited porous Si

Minoru Fujii,* Shingo Minobe, Motofumi Usui, and Shinji Hayashi
Department of Electrical and Electronics Engineering, Faculty of Engineering, Kobe University, Rokkodai, Nada, Kobe 657-8501, Japan

Egon Gross, Joachim Diener, and Dmitri Kovalev
Technische Universität München, Physik-Department, D-85747 Garching, Germany
(Received 1 April 2004; published 23 August 2004)

Photoluminescence (PL) from singlet oxygen generated by energy transfer from porous Si is observed at room temperature in an organic solvent. The evidence of the indirect excitation by energy transfer is obtained from PL excitation spectroscopy. The excitation spectrum indicates that by using porous Si as a photosensitizer, light of the entire visible range can be utilized for singlet oxygen generation at room temperature.

DOI: 10.1103/PhysRevB.70.085311 PACS number(s): 73.22.−f, 78.67.Bf, 78.55.Mb

I. INTRODUCTION

The molecule-like electronic structure of silicon (Si) nanocrystals [1–4] provides them with noble functions which have been realized so far by organic molecules. Very recently, Si nanocrystal assemblies, i.e., porous Si, are found to be an efficient photosensitizer for the formation of a kind of active oxygen species, called singlet oxygen ($^1O_2$).[5,6] Singlet oxygen representing electrically excited states of an oxygen molecule is a very important material in biology and chemistry because it mediates important processes in modification of biological structures.[7,8] Formation of singlet oxygen requires the presence of light-absorbing photosensitizer with subsequent energy transfer of electronic excitation to molecular oxygen. For efficient energy transfer photosensitizers must have spin-triplet excited states to satisfy the spin-conservation rule during the energy transfer process.[7] Furthermore, the lifetime of the excited triplet state should be long to enhance the probability of energy exchange.

Si nanocrystals satisfy all these criteria. Excitons confined in Si nanocrystals exhibit two electronic states; an optically active spin-singlet state and an optically inactive spin-triplet state which is lowered in energy. The singlet-triplet splitting increases with decreasing the nanocrystal size and is in milli electron-volt range for nanocrystals several nanometers in diameter.[1–4] Because of the small splitting energy, at room temperature these states are equally populated, and thus 75% of excitons reside in the threefold degenerated triplet state. The lifetime of the triplet state is of the order of milliseconds, while that of the singlet state is $10-100$ μs.[1–4] At room temperature excitons persist in the triplet state on a time scale comparable to the lifetime of the singlet state.[6]

From detailed optical studies of the system consisting of porous Si and oxygen molecules, it has been demonstrated that the triplet exciton in Si nanocrystals plays the same role as a triplet-excited state of dye molecules. Singlet oxygen is generated by exactly the same mechanism, i.e., energy transfer is realized by electron exchange between the triplet excited state of a sensitizer to the triplet ground state of an oxygen molecule, a process known as triplet-triplet annihilation.[5–7]

The formation of singlet oxygen is evidenced by photoluminescence (PL) measurements in the near-infrared spectral region where a narrow line ($\sim$0.98 eV) due to radiative relaxation of the lowest excited singlet state, $^1\Delta$, to the ground triplet state, $^3\Sigma$, of oxygen molecules is detected. However, because of the restriction of spin and angular momentum conservation rules, the oscillator strength of the transition is extremely small; the intrinsic lifetime of the $^1\Delta$ state is very long (2.7×10^3 s)[7] resulting in a very weak PL intensity. In our previous work,[5,6] the emission from singlet oxygen was detected only at very low temperatures when oxygen molecules are condensed on the surface of Si nanocrystals. At temperatures higher than the condensation temperature, i.e., $\sim$90 K, the emission was not detected and the formation of singlet oxygen was monitored only indirectly by analyzing the quenching of the PL from an energy donor, i.e., Si nanocrystals, under the assumption that the quenching is due to energy transfer from Si nanocrystals to oxygen molecules.

One of the standard methods to detect singlet oxygen at room temperature is to use a biochemical trap (singlet oxygen acceptor) and analyze a specific reaction product or monitor the decrease in the amount of the acceptor material. Typical biochemical traps are cholesterol, 1,3-diphenylisobenzofuran (DPBF), *p*-nitrosodimethylalanine, sodium azide, etc.[8,9] In our previous work,[10] we employed DPBF as a singlet oxygen acceptor. DPBF readily undergoes a 1,4-cycloaddition reaction with singlet oxygen forming endoperoxides, which decompose to yield irreversible products (1,2-dibenzoylbenzene). This process can be monitored by the decrease in the intensity of the absorption band of DPBF centered at 416 nm.[11,12] We have studied the absorption spectra of DPBF-dissolved solution containing porous Si powder under light irradiation and demonstrated that porous Si acts as a photosensitizer for singlet oxygen generation in solution at room temperature.[10]

However, these are indirect evidences and there still remains a room to dispute whether singlet oxygen is really generated by energy transfer from Si nanocrystals at room temperature or not. Therefore, the formation at room temperature must be proved without doubt by detecting the near-infrared emission from singlet oxygen.

Although the intrinsic radiative lifetime of $^1O_2$ in the lowest excited state, $^1O_2(^1\Delta)$, is extremely long, intermolecular interactions lead to an enhancement of the transition rate.[13] The radiative transition rate is three to four orders of magnitude larger in solution than in diluted gas phase.[13] However, in most solvents, deactivation of $^1O_2$ is radiationless by collisional electronic to vibrational energy transfer from $^1O_2$ to a solvent molecule; electronic excitation energy of $^1O_2$ is converted into vibrational energy of the ground state triplet oxygen $^3O_2(^3\Sigma)$ and a solvent molecule. The most probable energy-accepting oscillator of a solvent molecule is its terminal atom pairs with the highest vibrational energy (e.g., O-H, C-H).[14,15] Molecules composed of low energy oscillators such as C-F and C-Cl act as poor quenchers whereas those with high energy oscillators such as O-H and C-H are strong quenchers. In fact, the lifetime of $^1O_2(^1\Delta)$, varies over a wide range, from 4 μs to 100 ms, depending on the kind of solution.[14,15] Therefore, to obtain reliable luminescence data, solvents consisting of poor quenchers should be chosen. The second important requirement on the solvent is that it should not quench luminescence of porous Si.

As a solvent which satisfies these requirements, we employed hexafluorobenzene (C_6F_6). The singlet oxygen lifetime in the solution is about 25 msec,[14] which is about three orders of magnitude longer than that in benzene (C_6H_6). In this work, we study PL from porous Si powder dispersed in C_6H_6. From the PL studies, we demonstrate that singlet oxygen can be generated by the energy transfer from porous Si at room temperature.

II. EXPERIMENTAL PROCEDURE

As has been discussed in previous papers,[5,6] the ability of singlet oxygen formation depends strongly on the band gap energy of Si nanocrystals comprising porous Si. The efficiency of singlet oxygen formation is the highest for nanocrystals having a luminescence (band gap) energy of 1.63 eV, which corresponds to the energy separation of the second excited singlet state of oxygen molecules ($^1\Sigma$) and the triplet ground state ($^3\Sigma$); these nanocrystals can transfer resonantly their electronic excitation to oxygen molecules staying on the surface. If the bandgap energy is far from 1.63 eV, emission or absorption of phonons is required during the energy transfer process to conserve the energy. The participation of phonons significantly reduces the energy transfer rate.

The band gap energy of porous Si can be controlled by the resistivity of Si wafers, the etching current density, the concentration of hydrofluoric acid in etching solution, etc. [2] In this work, porous Si was prepared by electrochemical etching of a (100) oriented boron-doped bulk Si wafer with a resistivity of 11–15 Ω cm in a 55:45 by volume mixture of hydrofluoric acid (46 wt % in water) and ethanol. The current density and the etching time were 54 mA/cm^2 and 3 h, respectively. As will be shown later, porous Si prepared with this condition exhibits a PL peak at around 1.63 eV.

After the electrochemical etching process, porous Si layers were rinsed with ethanol several times to minimize the amount of residual fluorine. With this preparation condition, porous Si layers crack due to capillary forces and become powder during drying. The powder was then crushed in a mortar and put into a quartz cell ($1\times1\times4$ cm^3) filled with C_6F_6. Oxygen was not intentionally dissolved in C_6F_6. During PL measurements, the solution was continuously stirred by a magnetic stirrer (5×2 mm ϕ) to avoid aggregation of the powder. The cell was irradiated from the front surface and the PL was collected from the same surface. Schematic illustration of the experimental setup is shown in the inset of Fig. 1. The excitation source was an Ar ion laser (457.9, 488.0, and 514.5 nm), a continuous-wave (cw) solid state laser (532 nm), or a cw Ti-sapphire laser (690–850 nm). The excitation light was not focused by lens, and thus the spot size is rather large (3 mm ϕ). Since the solution was muddy and excitation light was strongly scattered by porous Si powder grains, the cell was nearly uniformly irradiated. PL spectra were recorded by using a single monochromator equipped with a liquid N_2 cooled InGaAs near-infrared diode array. The spectral response of the detection system was calibrated with the aid of a reference spectrum of a standard tungsten lamp. For the time response measurements, a 480.0 nm line of an optical parametric oscillator excited by a frequency-tripled Nd:Yttritium–aluminum–garnet laser was used as an excitation source. The pulse width, the power, and the repetition frequency were 5 ns, 400 μJ/cm^2, and 20 Hz, respectively. A multichannel scaler was used in obtaining decay curves. The overall time resolution of the system was better than 100 ns. All the measurements were made at room temperature.

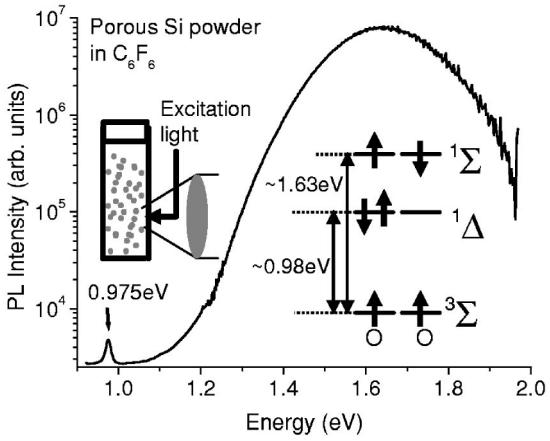

FIG. 1. PL spectrum of porous Si dispersed in C_6F_6 solution at room temperature. The peak at around 0.975 eV corresponds to the emission from singlet oxygen ($^1\Delta\rightarrow{}^3\Sigma$). Logarithmic scale is used for the vertical axis. The experimental setup and the energy diagram of an oxygen molecule are shown in the inset.

III. RESULTS AND DISCUSSION

Figure 1 shows the PL spectrum of porous Si powder (50 mg) dispersed in C_6F_6 solution (2 cm^3) at room temperature. The logarithmic scale is used for the vertical axis. The broad emission band centered at around 1.65 eV arises from the radiative recombination of excitons in Si nanocrystals assembling porous Si. In addition to the main PL band, a weak PL peak can be observed at around 0.975 eV. The peak

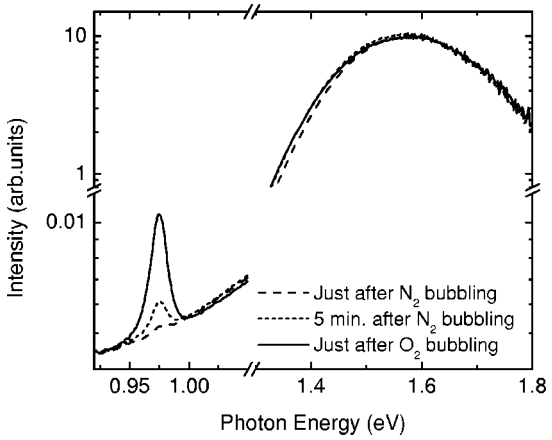

FIG. 2. PL spectra of porous Si dispersed in C_6F_6 solution at room temperature obtained just after bubbling with N_2 gas, 5 min after the N_2 gas bubbling, and just after bubbling with O_2 gas.

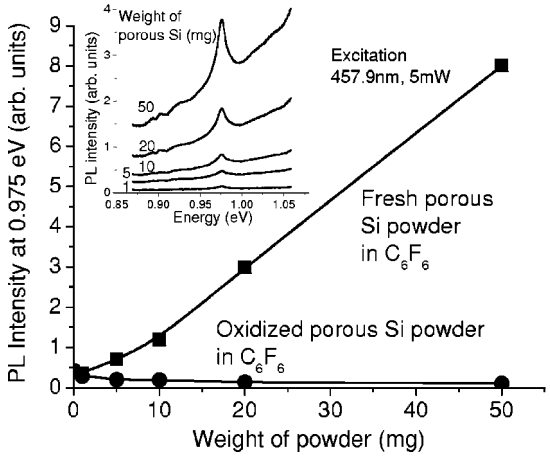

FIG. 3. PL intensity of singlet oxygen as a function of the amount of porous Si powder [fresh (■) and oxidized (•)] dispersed in C_6F_6. The intensities are obtained after subtracting a broad background signal from defects in porous Si. PL spectra are shown in the inset.

is very similar to that previously observed for porous Si at cryogenic temperatures when oxygen molecules are adsorbed.[5,6] In Fig. 2, PL spectra obtained after bubbling the solution with N_2 or O_2 gas are shown. In the spectrum measured just after N_2 gas bubbling, the 0.975 eV peak is missing, and it starts to appear several minutes after the bubbling. The peak becomes much larger when the solution is bubbled with O_2 gas. Thus, the 0.975 eV peak can be assigned to the radiative relaxation of $^1O_2(^1\Delta)$ dissolved in C_6F_6. It is worth noting that the 0.975 eV PL is not detected when benzene (C_6H_6) instead of C_6F_6 is used as solution, although the PL intensity of porous Si powder is nearly the same. Very efficient nonradiative relaxation of $^1O_2(^1\Delta)$ via energy transfer to the C-H vibration of benzene may be responsible for the disappearance of the PL.

To confirm the indirect excitation of oxygen molecules by the energy transfer from porous Si, PL spectra for the solution containing different amounts of porous Si powder are measured (inset in Fig. 3). With increasing the amount of powder, a broad background signal due to defect-related PL from porous Si grows which is accompanied by the growth of the 0.975 eV peak due to $^1O_2(^1\Delta)$. In Fig. 3, the PL intensity at 0.975 eV is plotted as a function of the weight of porous Si powder. To extract the intensity of the singlet oxygen PL the background PL from porous Si is subtracted. The squares in Fig. 3 represent the intensity obtained for the solution containing fresh hydrogen-terminated porous Si powder. The strong dependence of the intensity on the amount of porous Si is a clear evidence that the PL is excited by energy transfer from Si nanocrystals.

Since energy transfer is mediated by electron exchange, the efficiency depends strongly on the surface termination of Si nanocrystals. Even a monolayer of oxide on the surface significantly suppresses the singlet oxygen formation efficiency because the oxide layer acts as an energy barrier for electron exchange.[5,6] The circles in Fig. 3 represent the PL intensity at 0.975 eV obtained for the solution containing oxidized porous Si powder. The oxidation is made by immersing powder in distilled water for a few days. The PL intensity for the solution containing oxidized powder is much smaller than that containing fresh powder.

Another direct evidence of the photosensitized formation of singlet oxygen is obtained from PL excitation spectroscopy. In Fig. 4(a), PL spectra excited at different photon energies are plotted. In Fig. 4(b), the intensity of the singlet oxygen PL obtained by subtracting the broad background PL is plotted as a function of excitation energy (•). The excitation power is fixed to 200 mW for all energies. A logarithmic scale is used for the vertical axis. We can see that singlet oxygen is generated by light having a broad range of energies. This broad excitation spectrum is apparently different from that obtained for C_6F_6 not containing porous Si powder [□ in Fig. 4(b)]. In this case, singlet oxygen is generated by excitation light having an energy exactly resonant to the $^3\Sigma \rightarrow {}^1\Sigma$ transition. The broad excitation spectrum evidences the indirect excitation of singlet oxygen by energy transfer from porous Si.

In Fig. 4(b), the increase of the intensity at higher excitation energy can be explained qualitatively by the larger absorption coefficient of porous Si at higher energies. Furthermore, preferential energy transfer to the second excited $^1\Sigma$ state is responsible for the strong excitation energy dependence. The energy transfer to the $^1\Sigma$ state can be made resonantly without the participation of phonons if the band gap energy of Si nanocrystals coincides with the $^3\Sigma \rightarrow {}^1\Sigma$ transition energy. On the other hand, the energy transfer to the $^1\Delta$ state is always accompanied by the emission of multiple phonons in Si nanocrystals to satisfy the energy conservation rule. Because of the requirement of phonon emission and the restriction of the orbital angular momentum conservation ($\Delta L=2$ for $^3\Sigma \rightarrow {}^1\Delta$) during the energy transfer, the energy transfer rate to the $^1\Delta$ state is much smaller than that to the $^1\Sigma$ state. The energy transfer time to the $^1\Delta$ and $^1\Sigma$ states is estimated to be of the order of 100 μs and less than 3 μs, respectively, at cryogenic temperatures.[6] At room temperature, the very long energy transfer time to the $^1\Delta$ state results in a very small energy transfer efficiency because in most cases photoexcited electron-hole pairs recombine before

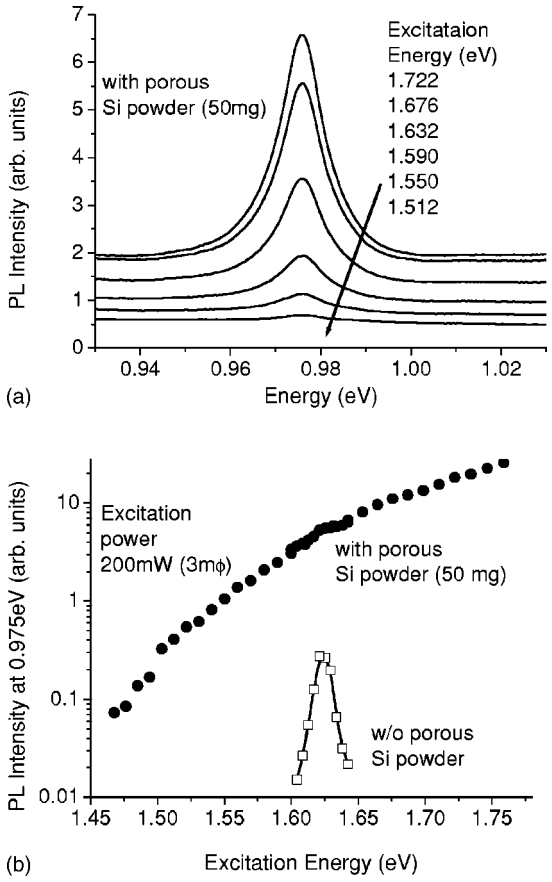

FIG. 4. (a) PL spectra of singlet oxygen excited at different energies. The flat background is due to defect-related PL of porous Si. (b) PL intensity of singlet oxygen as a function of excitation energy for C_6F_6 containing porous Si powder (•) and not containing porous Si powder (□). Logarithmic scale is used for the vertical axis. The intensity is obtained after subtracting a broad background signal from defects in porous Si. The excitation power was fixed to 200 mW for all excitation energies, because PL intensity does not linearly depend on excitation power.

transferring the energy to oxygen molecules. Therefore, only the energy transfer to the $^1\Sigma$ state is practically possible at room temperature. This results in the rapid decrease of the singlet oxygen formation efficiency below the $^3\Sigma \rightarrow {}^1\Sigma$ transition energy; Si nanocrystals having the band gap energy smaller than the $^3\Sigma \rightarrow {}^1\Sigma$ transition energy cannot contribute to singlet oxygen generation at room temperature. However, we do not see a clear onset exactly at the resonant energy. This is mainly due to thermal broadening of these states at room temperature. In fact, quenching of the PL from porous Si by transferring energy to oxygen molecules occurs in a rather wide spectral range; the full width at half maximum of the quenched region is about 300 meV at room temperature.[6]

After being excited to the $^1\Sigma$ state, $^1O_2(^1\Sigma)$ relaxes to $^1O_2(^1\Delta)$ radiatively or nonradiatively due to collisional electronic to vibrational energy transfer from $^1O_2(^1\Sigma)$ to a solvent molecule. The $^1\Delta$ excited state persists for a rather long time and finally relaxes to the ground $^3\Sigma$ state, resulting in the emission at 0.975 eV. The direct radiative relaxation of the $^1\Sigma$ state to the $^3\Sigma$ ground state may also be possible.

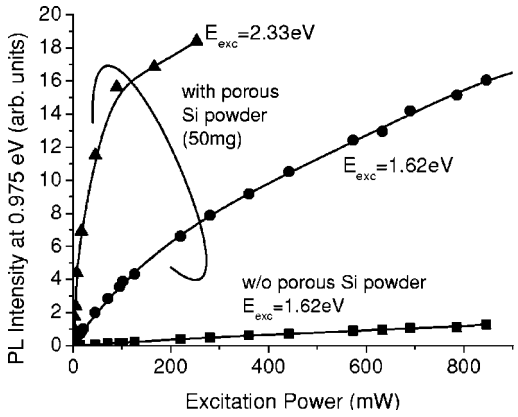

FIG. 5. Excitation power dependence of singlet oxygen PL intensity for C_6F_6 containing porous Si powder (▲: 2.33 eV excitation and •: 1.62 eV excitation) and not containing porous Si powder excited by 1.62 eV light (■).

However, the emission at 1.63 eV cannot be resolved because of the strong emission from porous Si.

In Fig. 5, the intensity of the singlet oxygen PL is plotted as a function of excitation power for the C_6F_6 solution containing and not containing porous Si powder. With porous Si powder excited by 2.33 and 1.62 eV light, the intensity saturates at very low excitation power, while without porous Si powder, it increases nearly linearly. The absorption coefficient of the $^3\Sigma \rightarrow {}^1\Sigma$ transition is extremely small even for resonant excitation. This results in a linear increase of the PL intensity. On the other hand, the strong saturation of the PL for the solution containing porous Si powder suggests that the energy transfer rate is much larger than the relaxation rate of $^1O_2(^1\Delta)$, and at high illumination levels almost all oxygen molecules are in the excited singlet state.

The lifetime of photogenerated singlet oxygen is deduced from the transient of the singlet oxygen emission. Figure 6 shows the PL decay curves. Since the singlet oxygen emis-

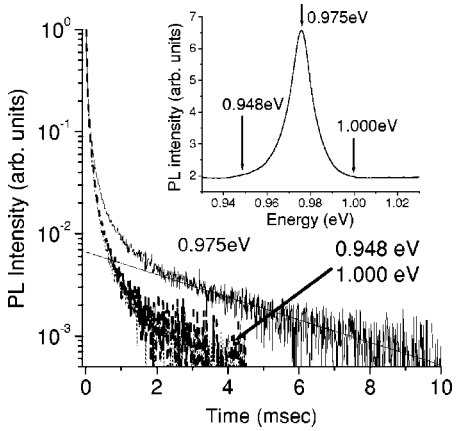

FIG. 6. PL decay curves detected at 0.948, 0.975, and 1.000 eV. Inset: Positions of the detection energies are indicated. The curve obtained at 0.975 eV consists of the fast decay due to the defect-related PL and the slow decay due to the singlet oxygen PL. The solid line is the result of the fitting of the slow component by a single exponential function. The decay time of the slow component is about 3.9 ms.

sion line is superimposed on a broad defect-related PL band, the decay curves are measured at the peak of the singlet oxygen PL line (0.975 eV) and at both sides of the peak (0.948 eV and 1.000 eV) (see the inset in Fig. 6). At the detection energy of 0.975 eV, a fast and a slow decay components are observed. The initial fast decay is attributed to the defect-related background PL, which can also be seen at detection energies of 0.948 and 1.000 eV. Thus, the slow component corresponds to the singlet oxygen PL. The lifetime estimated by fitting the slow component by a single exponential function is about 3.9 ms. This time is shorter than the value reported previously (25 ms).[14] A possible nonradiative relaxation channel responsible for the shortening of the lifetime may be the collisions of singlet oxygen with the walls of porous Si pores where the majority of singlet oxygen is generated.

IV. CONCLUSION

We succeeded in observing PL from singlet oxygen generated by the energy transfer from porous Si at room temperature. Because of the very broad absorption band of porous Si covering the entire visible range and a part of the near infrared range, singlet oxygen can be generated by light having a wide rage of energies starting from 1.5 eV. This is certainly an advantage compared to organic photosensitizers exhibiting usually a much narrower absorption band. The lifetime of generated singlet oxygen is shorter than that in pure C_6F_6 and is probably due to the collision with pore walls. The collision with pore walls enhances the relaxation rate of singlet oxygen making the extraction of generated singlet oxygen outside pores difficult. Therefore, for practical application of Si nanocrystals as a singlet oxygen generator, smaller grain size of porous Si powder or Si colloids are desirable. This issue requires further study.

ACKNOWLEDGMENT

This work is supported by Industrial Technology Research Grant Program in '03 from New Energy and Industrial Technology Development Organization (NEDO) Japan.

*Electronic address: fujii@eedept.kobe-u.ac.jp

[1] P. D. J. Calcott, K. J. Nash, L. T. Canham, M. J. Kane, and D. Brumhead, J. Phys.: Condens. Matter **5**, L91 (1993).
[2] A. G. Cullis, L. T. Canham, and P. D. J. Calcott, J. Appl. Phys. **82**, 909 (1997).
[3] D. Kovalev, H. Heckler, G. Polisski, and F. Koch, Phys. Status Solidi B **215**, 871 (1999).
[4] S. Takeoka, M. Fujii, and S. Hayashi, Phys. Rev. B **62**, 16 820 (2000).
[5] D. Kovalev, E. Gross, N. Künzner, F. Koch, V. Yu. Timoshenko, and M. Fujii, Phys. Rev. Lett. **89**, 137401 (2002).
[6] E. Gross, D. Kovalev, N. Künzner, J. Diener, F. Koch, V. Yu. Timoshenko, and M. Fujii, Phys. Rev. B **68**, 115405 (2003).
[7] N. J. Turro, *Modern Molecular Photochemistry* (University Science, Sausalito, CA, 1991).
[8] L. Packer and H. Sies, *Singlet Oxygen, UV-A, and Ozone* (Academic Press, London, 2000).
[9] D. B. Min and J. M. Boff, Chemistry and Reactions of Singlet Oxygen in Foods, Vol. 1, Comprehensive Reviews in Food Science and Food Safety **1**, 58 (2002).
[10] M. Fujii, M. Usui, S. Hayashi, E. Gross, D. Kovalev, N. Künzner, J. Diener, and V. Yu. Timoshenko, J. Appl. Phys. **95**, 3689 (2004).
[11] R. H. Young, K. Wehrly, and R. L. Martin, J. Am. Chem. Soc. **93**, 5774 (1971).
[12] M. Nowakowska, M. Kępczyński, and K. Szczubiatka, Macromol. Chem. Phys. **196**, 2073 (1995).
[13] M. Hild and R. Schmidt, J. Phys. Chem. A **103**, 6091 (1999).
[14] R. Schmidt, J. Am. Chem. Soc. **111**, 6983 (1989).
[15] R. Schmidt, F. Shafii, and M. Hild, J. Phys. Chem. **103**, 2599 (1999).